

# T2K EXPERIMENT NEUTRINO CROSS SECTIONS RESULTS\*

KAMIL PORWIT

on behalf of the T2K Collaboration

Institute of Physics, University of Silesia, Katowice, Poland

*(Received November 25, 2019)*

The understanding of neutrino–nucleus interactions is crucial for the precise measurement of neutrino oscillations phenomenon. Moreover, it is important for Monte Carlo modeling of neutrinos interactions, which at this moment is simplified. For this reason, a variety of cross-section measurements on different target materials and at different neutrino beam energies are performed worldwide. The goal of this paper is to review the recent results from neutrino cross-section measurements from the T2K experiment.

DOI:10.5506/APhysPolB.50.1749

## 1. Introduction

Neutrinos are most elusive particles in the Standard Model. They were first detected in 1956, what is now known as the Cowan–Reines experiment. Inverse  $\beta$ -decay reaction was used for the anti-neutrino event detection. For neutrino detection, massive flux of particles should be delivered. Such requirements were fulfilled near a nuclear reactor which brought  $5 \times 10^{13} \frac{\bar{\nu}_e}{\text{s cm}^2}$  [1]. On average, three anti-neutrino interactions per hour were detected. Measured cross section was established as  $6.3 \times 10^{-44} \text{ cm}^2$  [2] which illustrates how unwillingly neutrinos interact with matter.

Over time, more and more sophisticated methods were used to measure neutrino cross sections. The T2K experiment [3] uses near detectors for that purpose. The near-detector complex is situated 280 m from the neutrino interaction target. It consists of two near detectors. The first detector called INGRID [4] is placed at the center of neutrino beam (on-axis). It is made of 16 modules, each consisting of a sandwich structure of nine iron

---

\* Presented by K. Porwit at the XLIII International Conference of Theoretical Physics “Matter to the Deepest”, Chorzów, Poland, September 1–6, 2019.

target plates and 11 tracking scintillator planes, and one extra module which is made of plastic scintillators only. The main purpose of this detector is to monitor stability, direction and intensity of the J-PARC neutrino beam. The second near detector called ND280 is placed  $2.5^\circ$  off axis. It consists of several subdetectors placed in 0.2 T magnetic field. Two Fine Grained Detectors (FGD) [5] are essential for the cross-section measurements. FGD1 is built of plastic scintillators layers only, while FGD2 has also water layers between plastic scintillators. Both near detectors are shown in Fig. 1.

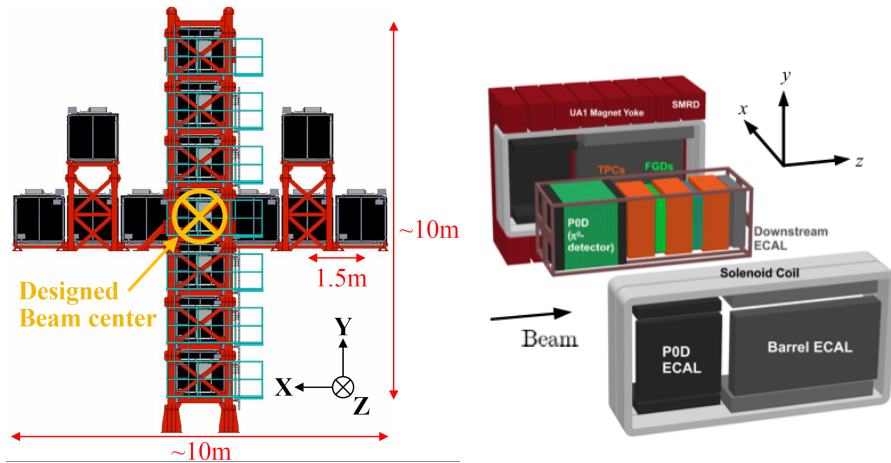


Fig. 1. Near detectors of the T2K experiment: INGRID detector left, ND280 detector right [3].

The far detector of the T2K experiment, Super-Kamiokande (SK) [6], is situated 295 km from the interaction target. It is filled with 50 kton of water where the neutrino interactions are registered exploiting Cherenkov effect. Configuration and composition of near detectors allow to measure a variety of neutrino cross sections. As the ND280 and SK detectors are different (material, angular acceptance), the neutrino interaction model is used to extrapolate the near-detector spectrum to the far-detector spectrum. Therefore, precise measurements of neutrino cross sections on different target materials and at different neutrino energies test neutrino interaction models, and they are an important ingredient for oscillation measurements.

## 2. Cross-sections measurements at T2K

### 2.1. $\nu_e CC$ and $\bar{\nu}_e CC$ inclusive cross section on plastic

Measurement of the  $\nu_\mu$  disappearance and  $\nu_e$  appearance at the far detector is affected by intrinsic  $\nu_e$  contamination in the  $\nu_\mu$  beam. Therefore,

correct understanding of  $\nu_e$  interactions is particularly important and near detectors can be useful for that purpose. However, selection of  $\nu_e$  events in the ND280 detector is challenging. The number of electrons from  $\nu_e$  charge current (CC) interactions is small compared to the number of muons coming from  $\nu_\mu$  CC events. Moreover, electrons coming from other sources, such as  $\pi^0$  decay, can mimic electrons coming from  $\nu_e$  interactions. Furthermore, measurement of the  $\nu_e(\bar{\nu}_e)$  cross section can test the interaction models which were mainly tuned for the  $\nu_\mu$  measurements.

The CC electron-neutrino interaction signal is defined by selection of primary electron occurring in FGD fiducial volume (FV). Any  $\nu_e$  CC event which happened outside FGD FV, but was mis-reconstructed as an event inside FGD FV is classified as a background. The gamma background consists of events with gamma conversion point inside the FGD FV. The event selection is divided into two parts. Firstly, the large muon, pion and proton backgrounds are rejected, thanks to excellent particle identification (PID) in the Time Projection Chambers of the ND280 detector. Secondly, gamma control sample which constrains the gamma background is selected.

For the  $\nu_e$  CC event selection in FGD1 FV, data from runs 2–4, 7c and 8 were used. This corresponds to  $11.92 \times 10^{20}$  protons on target (POT). The Monte Carlo (MC) sample was generated with *Neut* [7]. A total number of  $12.0801 \times 10^{21}$  MC POT was generated. Runs 5–7b were used for the  $\bar{\nu}_e$  CC event selection in FGD1, corresponding to  $6.2942 \times 10^{20}$  POT, whereas *Neut* MC sample corresponds to  $6.489 \times 10^{21}$  MC POT. The selection applied to the data and MC sets has resulted in 697  $\nu_e$  CC inclusive data events and 797.07 MC events with 26.2% efficiency and 53.7% purity. For the  $\bar{\nu}_e$  CC inclusive events, 176 data events and 175.95 MC events with 32.8% efficiency and 47.5% purity were selected. The selected signal breakdown is presented in Table I.

TABLE I

Event breakdown of the CC- $\nu_e$  inclusive selection in FGD1.

Beam mode	$\nu_e$ CC $0\pi$	$\nu_e$ CC-other	$\gamma$ bckg.	$\mu^\pm$ bckg.	Other bckg.
$\nu_\mu$ -mode	199.75 (25.06%)	229.41 (28.78%)	240.32 (30.15%)	35.67 (4.47%)	91.92 (11.53%)
$\bar{\nu}_\mu$ -mode	33.43 (19.00%)	50.19 (28.53%)	62.64 (35.61%)	6.38 (3.63%)	23.28 (13.23%)

The likelihood fit to the data was performed to extract cross-section results. Moreover, results were re-calculated using *Genie* MC generator. The total post-fit data-MC  $\chi^2$  is 1.02 for *Genie* and 1.50 for *Neut* fit. The results are shown in Fig. 2, whereas the total cross-section results for full phase space are presented in Table II.

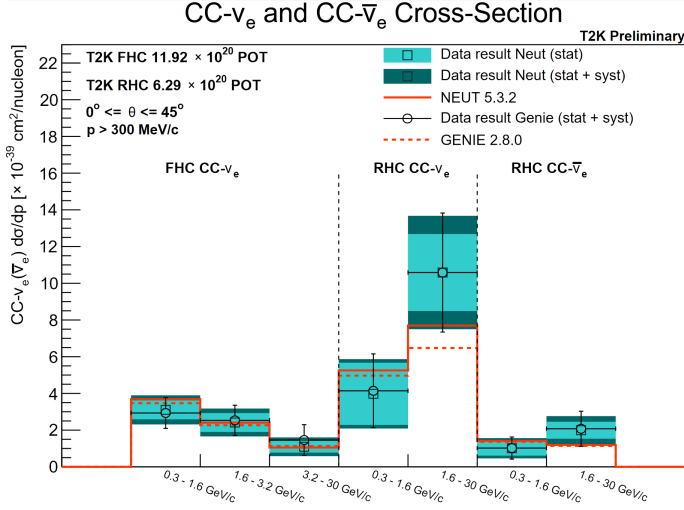


Fig. 2. T2K  $\nu_e$  CC and  $\bar{\nu}_e$  CC inclusive cross-section results obtained with Genie and Neut MC samples. FHC corresponds to the  $\nu_\mu$  beam mode and RHC corresponds to the  $\bar{\nu}_\mu$  beam mode.

TABLE II

T2K  $\nu_e$  CC and  $\bar{\nu}_e$  CC inclusive total cross sections  $\sigma$  extrapolated from the limited phase-space to full phase space using Neut and Genie MC. All  $\sigma$  values have  $\left[ \frac{10^{-39} \text{ cm}^2}{\text{nucleon}} \right]$  unit.

Beam mode	Channel	Neut $\sigma$	Neut $\sigma$	Genie $\sigma$	Genie $\sigma$
$\nu_\mu$ -mode	CC- $\nu_e$	10.21	11.02	10.57	10.48
		$\pm 2.05(\text{stat.})$ $\pm 1.95(\text{syst.})$		$\pm 2.36(\text{stat.})$ $\pm 1.64(\text{syst.})$	
$\bar{\nu}_\mu$ -mode	CC- $\nu_e$	19.55	17.36	19.98	15.29
		$\pm 6.35(\text{stat.})$ $\pm 3.65(\text{syst.})$		$\pm 7.09(\text{stat.})$ $\pm 2.07(\text{syst.})$	
$\bar{\nu}_\mu$ -mode	CC- $\bar{\nu}_e$	3.59	3.12	3.72	3.01
		$\pm 1.57(\text{stat.})$ $\pm 0.57(\text{syst.})$		$\pm 1.83(\text{stat.})$ $\pm 0.67(\text{syst.})$	

## 2.2. $\nu_\mu$ CC $0\pi$ flux integrated cross section ( $O$ , $C$ , $O/C$ )

The Charged Current Quasi Elastic (CCQE) process ( $\nu_\mu + n \rightarrow \mu^- + p$ ) is a dominant interaction up to 1 GeV neutrino energy. For the T2K experiment, in which  $\nu_\mu$  ( $\bar{\nu}_\mu$ ) flux peaks at  $\sim 600$  MeV, it is the main signal exploited to distinguish the flavor of neutrino interaction. Moreover, this process allows to reconstruct neutrino energy.

Five signal samples with muon and one or more protons, and two control samples with single-pion or multi-pion production are defined in this analysis. Control samples were used to constrain the CC non-Quasi Elastic events. As this analysis searches for interactions on oxygen and carbon, the event selection was conducted for the FGD1 and FGD2 FV's. Data from runs 2–4 were used corresponding to  $5.734 \times 10^{20}$  POT. The Neut MC with  $9.627 \times 10^{21}$  MCPOT was used. The purity and the number of selected events can be found in Table III.

TABLE III

Sample purity and number of selected events for all signal and control samples for T2K CCQE  $\nu_\mu$  cross-section measurements.

Sample	FGD	Purity [%]	Num. of events
All signal samples (CC0 $\pi$ )	1	87.4	12596
	2	81.8	11690
Control sample 1 (CC1 $\pi$ )	1	70.9	963
	2	63.2	1326
Control sample 2 (CC-other)	1	70.5	1588
	2	69.5	1592

To evaluate the statistical and systematic uncertainties, toy-throws experiments were performed. 1000 toy-fits are performed sampling the prior covariance matrix and response functions that describes all possible systematics. Each toy prior is then used to perform the fit to the data. The ex-

TABLE IV

CC0 $\pi$  cross sections per nucleon integrated over the muon kinematics for oxygen, carbon and their ratio. All  $\sigma$  values are in  $\left[ \frac{10^{-39} \text{ cm}^2}{\text{nucleon}} \right]$ .

Channel	Obtained $\sigma$	Neut $\sigma$	Genie $\sigma$
CC0 $\pi_{\text{O}}$	5.28	4.4	4.1
	$\pm 0.66(\text{stat.} + \text{syst.})$		
	$\pm 0.16(\text{bwd. migr.})$		
	$\pm 0.14(\text{pFSI})$		
CC0 $\pi_{\text{C}}$	4.72	4.7	4.2
	$\pm 0.57(\text{stat.} + \text{syst.})$		
	$\pm 0.14(\text{bwd. migr.})$		
	$\pm 0.12(\text{pFSI})$		
CC0 $\pi_{(\text{O/C})}$	1.12	1.06	1.03
	$\pm 0.08(\text{stat.} + \text{syst.})$		

tracted double differential cross section is obtained as a mean from the 1000 results and the standard deviation is taken as a global uncertainty. Moreover, proton Final State Interaction systematics (pFSI) and backward migrating tracks systematics (bwd. migr.) are evaluated and added in quadrature. The backward migrating tracks can happen when a low energetic particle, produced in the interaction, travels backward leaving some hits which are fitted together with the forward muon candidate, or when the muon candidate itself is backward. Obtained results can be found in Table IV, whereas the measured differential  $\nu_\mu$  cross section carbon oxygen ratio is presented in Fig. 3.

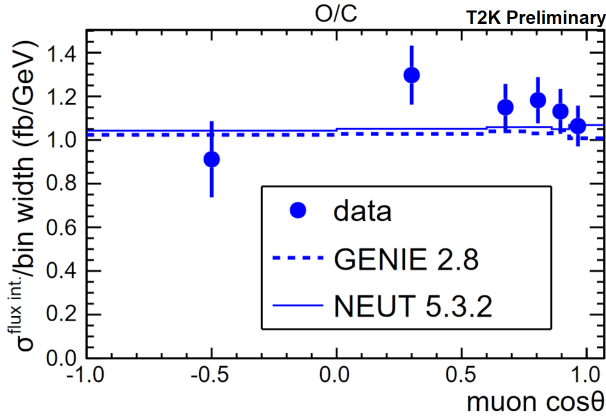


Fig. 3. The O/C differential cross section ratio as a function of  $\cos(\theta_\mu)$ , obtained by integrating the double differential cross section in each angle bin for 1000 toys. Data (dots) are compared with Neut (solid line) and Genie (dashed line).

### 2.3. $\bar{\nu}_\mu CC0\pi0p$ cross section on $H_2O$ and $CH$

To test the interaction model for the different neutrino types and energies the analysis of  $\bar{\nu}_\mu CC$  with neither pions nor protons ( $CC0\pi0p$ ) in the final state at  $1.5^\circ$  off-axis angle, which corresponds to 0.86 MeV beam mean energy was performed. For this off-axis angle the WAGASCI detector [8] which is a water target neutrino detector, and Proton Module [9] which is a plastic scintillator target detector were used. The INGRID module was used only as a muon-range detector. Configuration of these detectors is presented in Fig. 4.

The signal is defined as CC muon–anti-neutrino interaction, if the reconstructed muon momentum is larger than 0.4 GeV/c and the muon angle is smaller than  $30^\circ$  relative to the beam axis. Monte Carlo study showed that such conditions are required by the limited detector acceptance. To increase

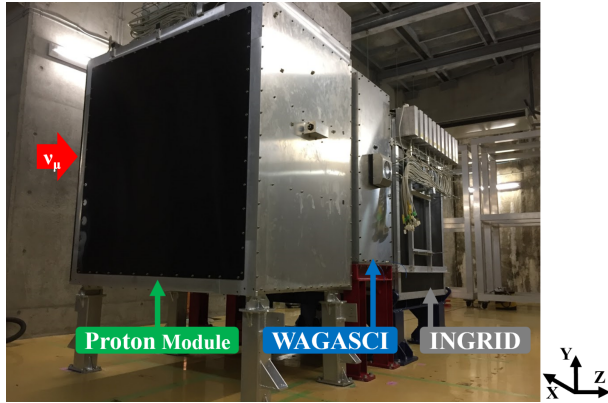


Fig. 4. Installed detectors at the B2 floor in the J-PARC neutrino monitor building. The beam axis corresponds to the  $Z$  axis.

the number of signal events and reduce the number of background events, the event selection was performed for WAGASCI and Proton Module detectors. In WAGASCI, selected events were divided into three categories: single-muon track forward, single-muon track backward and multi-muon tracks. The main signal corresponds to single-muon track forward sample. The samples are separated into six bins (every  $5^\circ$  in the range of  $0^\circ \div 30^\circ$ ) based on the reconstructed muon angle. Each selected track was matched with the tracks reconstructed in other detectors. Dedicated timing cuts, together with two- and three-dimensional track reconstructions ensured that the track belongs to the same event. Similar procedure was applied for tracks selected in Proton Module (PM). As PM is placed between WAGASCI and INGRID, the tracks were matched to both detectors. Summary of the event selection can be found in Table V.

TABLE V

Summary of the event  $\bar{\nu}_\mu$  CC0 $\pi$ 0 $p$  selection for WAGASCI and Proton Module.

Det.	$\bar{\nu}_\mu$	$\nu_\mu$	$\bar{\nu}_\mu + \nu_\mu$	External bckg.
WAGASCI	969.5(76.8%)	203.5(16.1%)	16.5(1.3%)	72.3(5.7%)
PM	1514.5(76.4%)	390.1(19.7%)	23.7(1.2%)	54.8(2.8%)

The  $\bar{\nu}_\mu$  (and  $\bar{\nu}_\mu + \nu_\mu$ ) CC0 $\pi$ 0 $p$  cross sections on H<sub>2</sub>O and CH are calculated from the number of selected events in WAGASCI and Proton Module. In addition, the Proton Module was used for the statistical subtraction of neutrino interactions on the WAGASCI scintillators. The integrated cross section for the muon angles from 0 to 30 degrees is shown in Table VI.

TABLE VI

CC0 $\pi$ 0 $p$  cross sections per nucleon integrated over muon angles from 0° to 30° for H<sub>2</sub>O, CH and their ratios. All  $\sigma$  values are in  $\left[ \frac{10^{-39} \text{ cm}^2}{\text{nucleon}} \right]$ .

Channel	Obtained $\sigma$	Neut $\sigma$
$\bar{\nu}_\mu \text{CC}0\pi 0p_{\text{H}_2\text{O}}$	$1.082 \pm 0.068(\text{stat.})^{+0.145}_{-0.128}(\text{syst.})$	1.024
$\bar{\nu}_\mu \text{CC}0\pi 0p_{\text{CH}}$	$1.096 \pm 0.054(\text{stat.})^{+0.132}_{-0.117}(\text{syst.})$	1.062
$\bar{\nu}_\mu \text{CC}0\pi 0p_{(\text{H}_2\text{O}/\text{CH})}$	$0.987 \pm 0.078(\text{stat.})^{+0.093}_{-0.090}(\text{syst.})$	0.964
$(\bar{\nu}_\mu + \nu_\mu) \text{CC}0\pi 0p_{\text{H}_2\text{O}}$	$1.155 \pm 0.064(\text{stat.})^{+0.148}_{-0.129}(\text{syst.})$	1.094
$(\bar{\nu}_\mu + \nu_\mu) \text{CC}0\pi 0p_{\text{CH}}$	$1.159 \pm 0.049(\text{stat.})^{+0.129}_{-0.115}(\text{syst.})$	1.139
$(\bar{\nu}_\mu + \nu_\mu) \text{CC}0\pi 0p_{(\text{H}_2\text{O}/\text{CH})}$	$0.996 \pm 0.069(\text{stat.})^{+0.083}_{-0.078}(\text{syst.})$	0.960

### 3. Summary

Measurements of neutrino–nucleus cross sections are essential to increase the precision of the determination of neutrino oscillations parameters. Such measurements are an important input to the Monte Carlo modeling of the neutrino interactions, which are still simplified. Furthermore, it is still not clear what models should be used for proper description of all available cross-section measurements. Thus, the measurements should be performed in a model-independent way and should be compared with other available cross-section results. In this paper, the T2K experiment measurements of neutrino cross section on a variety of target materials and for different off-axis angles corresponding to different  $\nu_\mu(\bar{\nu}_\mu)$  energy peaks, were presented.

This work was supported by the Ministry of Science and Higher Education, Poland, DIR/WK/2017/05.

### REFERENCES

- [1] D.J. Griffiths, *Introduction to Elementary Particles*, John Wiley & Sons, 1987.
- [2] C.L. Cowan *et al.*, *Science* **124**, 103 (1956).
- [3] K. Abe *et al.*, *Nucl. Instrum. Methods Phys. Res. A* **659**, 106 (2011).
- [4] K. Abe *et al.*, *Nucl. Instrum. Methods Phys. Res. A* **694**, 211 (2012).
- [5] P.A. Amaudruz *et al.*, *Nucl. Instrum. Methods Phys. Res. A* **696**, 1 (2012).
- [6] Y. Fukuda *et al.*, *Nucl. Instrum. Methods Phys. Res. A* **501**, 418 (2003).
- [7] Y. Hayato, *Nucl. Phys. B Proc. Suppl.* **112**, 171 (2002).
- [8] B. Quilain, A. Minamino, *J. Phys.: Conf. Ser.* **888**, 012166 (2017).
- [9] K. Abe *et al.*, *Phys. Rev. D* **90**, 052010 (2014).